Journal of Photochemistry and Photobiology B: Biology 130 (2014) 205–216

Contents lists available at ScienceDirect

Journal of Photochemistry and Photobiology B: Biology

journal homepage: www.elsevier.com/locate/jphotobiol

Synthesis, characterization and crystal structure of cobalt(III) complexes containing 2-acetylpyridine thiosemicarbazones: DNA/protein interaction, radical scavenging and cytotoxic activities

Rajendran Manikandan [a], Periasamy Viswanathamurthi [a,*], Krishnaswamy Velmurugan [b], Raju Nandhakumar [b], Takeshi Hashimoto [c], Akira Endo [c]

[a] Department of Chemistry, Periyar University, Salem 636011, Tamil Nadu, India
[b] Department of Chemistry, Karunya University, Karunya Nagar, Coimbatore 641 114, India
[c] Department of Materials and Life Sciences, Sophia University, Tokyo 102-8554, Japan

ARTICLE INFO

Article history:
Received 7 October 2013
Received in revised form 6 November 2013
Accepted 11 November 2013
Available online 22 November 2013

Keywords:
Cobalt(III) complexes
DNA binding
DNA cleavage
Protein binding
Antioxidant activity
Cytotoxicity

ABSTRACT

The synthesis, structure and biological studies of cobalt(III) complexes supported by NNS-tridentate ligands are reported. Reactions of 2-acetylpyridine N-substituted thiosemicarbazone (HL^{1-3}) with $[CoCl_2(PPh_3)_2]$ resulted $[Co(L^{1-3})_2]Cl$ (**1**–**3**) which were characterized by elemental analysis and various spectral studies. The molecular structure of the complex **1** has been determined by single crystal X-ray diffraction studies. *In vitro* DNA binding studies of complexes **1**–**3** carried out by fluorescence studies and the results revealed the binding of complexes to DNA via intercalation. The binding constant (K_b) values of complexes **1**–**3** from fluorescence experiments showed that the complex **3** has greater binding propensity for DNA. The DNA cleavage activity of the complexes **1** and **3** were ascertained by gel electrophoresis assay which revealed that the complexes are good DNA cleavage agents. Further, the interactions of the complexes with bovine serum albumin (BSA) were also investigated using fluorescence spectroscopic method, which showed that the complexes **1**–**3** could bind strongly with BSA. The antioxidant property of the complexes was evaluated to test their free-radical scavenging ability. Furthermore, *in vitro* cytotoxicity of the complexes against MCF-7 and A431 cell lines was assayed which showed higher activity and efficiently vanished the cancer cells even at low concentrations.

1. Introduction

Cancer is undoubtedly one of the main health concerns facing our society and one of the primary targets regarding medicinal chemistry. Even though platinum-based complexes had been in the primary focus of research on chemotherapy agents [1–3], the interests in this field have shifted to non-platinum based agents [4–11], in order to find different metal complexes with less side effects and similar, or better, cytotoxicity. Thus, a wide variety of metal complexes based on titanium, gallium, germanium, palladium, gold, copper, nickel, ruthenium and tin are being intensively studied as platinum replacements [4–13].

Cobalt is an essential trace element in human, exhibiting many useful biological functions. Numerous compounds, naturally occurring and man-made, contain the cobalt at two common oxidation states Co(II) and Co(III). There is growing interest in investigating the cobalt and other transition metal complexes for their interaction with DNA [14–18]. Moreover, cobalt complexes appear to be very promising candidates for anticancer therapy; an idea supported by a considerable number of research articles describing the synthesis and cytotoxic activities of numerous cobalt complexes [19–26].

In addition, thiosemicarbazones are considered as an important class of nitrogen–sulfur donor ligands because of their highly interesting chemical, biological and medicinal properties, such as DNA binding, antioxidant, antibacterial, antiproliferative, antimalarial, anticancer and antitumor [27–33]. The presence of substituents at the 4-position have been shown to affect the activity of thiosemicarbazones and their metal complexes [34]. For example, metal complexes of 2-acetylpyridine thiosemicarbazones are found to exhibit increased antineoplastic activity when the N atom in the 4-position is part of a hexamethyleneiminyl ring instead of being a propyl- or dipropyl-carrying amine group [9]. The variable coordination behavior of thiosemicarbazone ligands towards transition metals, as well as antitumor activity of the resulting complexes are studied by West et al. [35–38]. We have previously reported the synthesis and biological studies of cadmium(II) complexes from 2-acetylpyridine thiosemicarbazones [39].

* Corresponding author. Fax: +91 427 2345124.
E-mail address: viswanathamurthi72@gmail.com (P. Viswanathamurthi).

1011-1344/$ - see front matter © 2013 Elsevier B.V. All rights reserved.
http://dx.doi.org/10.1016/j.jphotobiol.2013.11.008

In this study, the complexes of 2-acetylpyridine N-substituted thiosemicarbazone with Co(III) have been synthesized and characterized. The interactions of the complexes with CT-DNA/protein were investigated by using fluorescence spectroscopy. The DNA cleavage ability has been monitored by using gel electrophoresis experiment in the presence of the complexes using pBR322 DNA. The free radical scavenging ability, assays by a series of antioxidant assays involving DPPH, hydroxyl and nitric oxide radical. *In vitro* cytotoxic activities of the complexes were tested by MTT assays against human breast cancer cell line (MCF-7) and human skin carcinoma cell line (A431). The synthetic routes for the ligands and complexes are shown in Scheme 1.

2. Experimental

2.1. Materials and methods

All the reagents used were chemically pure and AR grade. The solvents were purified and dried according to standard procedures. $CoCl_2{\cdot}6H_2O$, calf-thymus DNA (CT-DNA), methylene blue (MB) and bovine serum albumin (BSA) were purchased from Sigma-Aldrich and used as received. The pBR322 DNA was purchased from Bangalore GeNei, Bangalore, India. The human breast cancer cell line (MCF-7) and human skin carcinoma cell line (A431) was obtained from National Centre for Cell Science (NCCS), Pune, India and grown in Dulbeccos Modified Eagles Medium (DMEM) containing 10% fetal bovine serum (FBS). Cells were maintained at 37 °C, 5% CO_2, 95% air and 100% relative humidity. Maintenance cultures were passaged weekly, and the culture medium was changed twice a week.

2.2. Physical measurements

Microanalyses of carbon, hydrogen, nitrogen and sulfur were carried out using Vario EL III Elemental analyzer at SAIF – Cochin, India. The IR spectra of the ligand and their complexes were obtained as KBr pellets on a Nicolet Avatar model spectrophotometer at 4000–400 cm^{-1} range. Electronic spectra of the ligand and their complexes have been recorded in acetonitrile using a Shimadzu UV-1650 PC spectrophotometer at 800–200 nm range. Emission spectra were measured with a Jasco FP 6600 spectrofluorometer. ^1H NMR spectra were recorded in Jeol GSX-400 instrument at room temperature using tetramethylsilane as the internal standard in dimethylsulfoxide (DMSO-d_6) as solvent. The ESI-MS spectra were recorded by using LC-MS Q-ToF Micro-analyzer (Shimadzu) in the SAIF, Panjab University, Chandigarh. Melting points were checked on a Technico micro-heating table and are uncorrected. The requisite precursor metal complex $[CoCl_2(PPh_3)_2]$ were prepared according to the literature method [40].

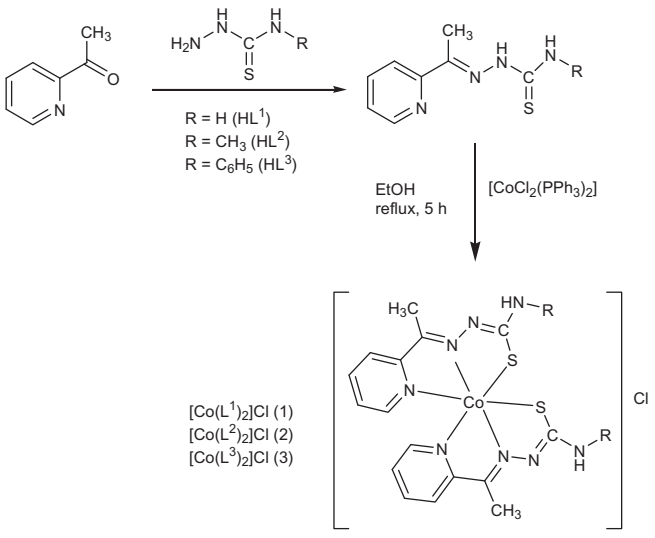

Scheme 1. Preparation of ligands and corresponding cobalt(III) complexes.

2.3. Synthesis of Schiff base ligands

The Schiff base ligands were prepared by condensation of equimolar amounts of 2-acetylpyridine (2 mmol) and substituted thiosemicarbazide (2 mmol) in ethanol (20 mL) under reflux for 5 h. Then the reaction mixture was cooled to room temperature, the yellow solid was separated, filtered off, washed with ethanol and dried in *vacuo* [41,42].

2.3.1. 2-Acetylpyridine-thiosemicarbazone (HL^1)

The ligand was obtained from the reaction of 2-acetylpyridine (0.22 mL; 2 mmol) and thiosemicarbazide (0.1822 g; 2 mmol). Yield: 0.3104 g, 80%; Color: yellow solid; M.p.: 180 °C; Anal. Calcd. for $C_8H_{10}N_4S$ (194.25 g mol^{-1}): C, 49.46; H, 5.18; N, 28.84; S, 16.50%. Found: C, 49.32; H, 5.26; N, 28.69; S, 16.32%. IR (KBr, cm^{-1}): 3373, 3260(m) ν(—NH—R), 3183(m) ν(NH), 1609(s) ν(C=N), 1583(s) ν(C=N), 836(m) ν(C=S). UV-Vis (CH_3CN, λ/nm (ε/M^{-1} cm^{-1})): 310 (46,064), 202 (32,588). ^1H NMR (300 MHz, DMSO-d_6, δ, ppm): 10.31 (s, 1H, NH); 8.19 (s, 2H, NH_2); 8.59–8.38 & 7.79–7.35 (m, 4H, aromatic); 2.38 (s, 3H, CH_3).

2.3.2. 2-Acetylpyridine-4-methyl-thiosemicarbazone (HL^2)

The ligand was obtained from the reaction of 2-acetylpyridine (0.22 mL; 2 mmol) and 4-methyl-thiosemicarbazide (0.2103 g; 2 mmol). Yield: 0.3038 g, 73%; Color: yellow solid; M.p.: 170 °C; Anal. Calcd. for $C_9H_{12}N_4S$ (208.28 g, mol^{-1}): C, 51.90; H, 5.80; N, 26.90; S, 15.39%. Found: C, 51.78; H, 5.72; N, 26.29; S, 15.78%. IR (KBr, cm^{-1}): 3289(m) ν(—NH—R), 3240(m) ν(NH), 1613(s) ν(C=N), 1578(s) ν(C=N), 834(m) ν(C=S). UV–Vis (CH_3CN, λ/nm (ε/M^{-1} cm^{-1})): 310 (44,364), 203 (30,211). ^1H NMR (300 MHz, DMSO-d_6, δ, ppm): 10.38 (s, 1H, NH); 8.65 (s, 1H, NH-R); 8.58–8.41 & 7.81–7.35 (m, 4H, aromatic); 3.08 (s, 3H, CH_3), 2.36 (s, 3H, CH_3).

2.3.3. 2-Acetylpyridine-4-phenyl-thiosemicarbazone (HL^3)

The ligand was obtained from the reaction 2-acetylpyridine (0.22 mL; 2 mmol) and 4-pheyl-thiosemicarbazide (0.3344 g; 2 mmol). Yield: 0.4324 g, 80%; Color: yellow solid; M.p.: 185 °C; Anal. Calcd. for $C_{14}H_{14}N_4S$ (270.35 g, mol^{-1}): C, 62.19; H, 5.21; N, 20.72; S, 11.85%. Found: C, 62.46; H, 5.56; N, 26.54; S, 11.63%. IR (KBr, cm^{-1}): 3301(m) ν(—NH—R), 3241(m) ν(NH), 1598(s) ν(C=N), 1580(s) ν(C=N), 801(m) ν(C=S). UV–Vis (CH_3CN, λ/nm (ε/M^{-1} cm^{-1})): 341 (18,249), 309 (15,890), 297 (16,657), 226 (22,190). ^1H NMR (300 MHz, DMSO-d_6, δ, ppm): 10.65 (s, 1H, NH); 10.25 (s, 1H, NH-R); 8.61–8.49 & 7.85–7.21 (m, 9H, aromatic); 2.40 (s, 3H, CH_3).

2.4. Synthesis of cobalt(III) Schiff base complexes

All the new metal complexes were prepared according to the following general procedure. A warm ethanolic solution (10 mL) containing Schiff base ligand (1 mmol) was added to an ethanolic solution of (10 mL) $[CoCl_2(PPh_3)_2]$ (1 mmol). The resulting red color solution was refluxed for 5 h. Dark red colored crystalline powder was obtained on slow evaporation. They were filtered off, washed with ethanol, and dried under *vacuo*.

2.4.1. Synthesis of $[Co(L^1)_2]Cl$ (1)

The complex was synthesized from $[CoCl_2(PPh_3)_2]$ (0.654 g; 1 mmol) and HL^1 (0.194 g; 1 mmol). Yield: 0.3991 g, 83%; Color: red solid; M.p.: 268 °C; Anal. Calcd. for $C_{16}H_{18}ClCoN_8S_2$ (480.89 g, mol^{-1}): C, 39.96; H, 3.77; N, 23.30; S, 13.33%. Found: C, 39.62; H, 3.43; N, 23.49; S, 13.13%. IR (KBr, cm^{-1}): 3376, 3256(m) ν(—NH—R), 1620(s) ν(C=N), 1598(s) ν(C=N), 1577(s) ν(C=N), 772(s) ν(C—S). UV–Vis (CH_3CN, λ/nm (ε/M^{-1} cm^{-1})): 402 (8465), 354 (13,900), 296 (28,090), 226 (47,859). ^1H NMR (300 MHz, DMSO-d_6, δ, ppm): 8.10 (s, 2H, NH_2); 8.09–7.44 (m, 4H, aromatic); 2.80 (s, 3H, CH_3). ESI-MS, m/z (%): 445.1 (85) $[M-Cl]^+$.

2.4.2. Synthesis of $[Co(L^2)_2]Cl$ (2)

The complex was synthesized from $[CoCl_2(PPh_3)_2]$ (0.654 g; 1 mmol) and HL^2 (0.208 g; 1 mmol). Yield: 0.402 g, 79%; Color: red solid; M.p.: 228 °C; Anal. Calcd. for $C_{18}H_{22}ClCoN_8S_2$ (508.94 g, mol^{-1}): C, 42.47; H, 4.36; N, 22.02; S, 12.60%. Found: C, 42.28; H, 4.72; N, 22.37; S, 12.91%. IR (KBr, cm^{-1}): 3248(w) ν(—NH—R), 1598(s) ν(C=N), 1579(s) ν(C=N), 1560(s) ν(C=N), 773(s) ν(C—S). UV–Vis (CH_3CN, λ/nm (ε/M^{-1} cm^{-1})): 418 (7430), 357 (8091), 302 (11,3486), 225 (21,882). ^1H NMR (300 MHz, DMSO-d_6, δ, ppm): 8.70 (s, 1H, NH-R); 7.82–7.78 & 7.61–7.41 (m, 4H, aromatic); 2.92 (s, 3H, CH_3), 2.37 (s, 3H, CH_3). ESI-MS, m/z (%): 473.1 (40) $[M-Cl]^+$.

2.4.3. Synthesis of $[Co(L^3)_2]Cl$ (3)

The complex was synthesized from $[CoCl_2(PPh_3)_2]$ (0.654 g; 1 mmol) and HL^3 (0.270 g; 1 mmol). Yield: 0.5317 g, 84%; Color: red solid; M.p.: 296 °C; Anal. Calcd. for $C_{28}H_{26}ClCoN_8S_2$ (633.08 g, mol^{-1}): C, 53.12; H, 4.14; N, 17.69; S, 10.13%. Found: C, 53.43; H, 4.38; N, 17.27; S, 10.54%. IR (KBr, cm^{-1}): 3389(m) ν(—NH—R), 1630(m) ν(C=N), 1599(s) ν(C=N), 1571(s) ν(C=N), 753(s) ν(C—S). UV–Vis (CH_3CN, λ/nm (ε/M^{-1} cm^{-1})): 420 (9873), 372 (15,696), 254 (27,848), 227 (35,443). ^1H NMR (300 MHz, DMSO-d_6, δ, ppm): 10.23 (s, 1H, NH-R); 8.68–8.52 & 7.84–7.25 (m, 9H, aromatic); 2.20 (s, 3H, CH_3). ESI-MS, m/z (%): 597.1 (60) $[M-Cl]^+$.

*2.5. X-ray structure determination of complex **1***

All data were obtained using a Rigaku Mercury CCD diffractometer with graphite monochromated Mo Kα radiation (k = 0.71070 Å). The structure was solved by direct methods and expanded using Fourier techniques [43,44]. All non-hydrogen atoms were refined anisotropically, using full-matrix least squares refinements on F^2 with crystal structure crystallographic software package [45]. Table 1 gives further details of data collection, refinement, and the structural details of complex $[Co(L^1)_2]$.

2.6. DNA binding and cleavage experiments

Luminescence measurement was performed to clarify the binding affinity of cobalt(III) complexes by emissive titration at room temperature. The complexes were dissolved in mixed solvent of 5% DMSO and 95% Tris–HCl buffer (5 mM Tris–HCl/50 mM NaCl buffer for pH = 7.2) for all the experiments and stored at 4 °C for further use and used within 4 days. Tris–HCl buffer was subtracted through base line correction. The excitation wavelength was fixed by the emission range and adjusted before measurements. Emissive titration experiments were performed with a fixed concentration of metal complexes (25 μM). While gradually increasing the concentration of DNA (0–25 μM), the emission spectra were monitored by keeping the excitation of the test compounds at 400 nm. MB-DNA experiments were conducted by adding the complexes to the Tris–HCl buffer of MB-DNA. The change in the fluorescence intensity was recorded. The excitation and emission wavelengths were 605 nm and 684 nm, respectively.

Table 1
Crystal data and structure refinement for the complex **1.**

Complex	**1**
Empirical formula	$C_{16}H_{18}ClCoN_8S_2$
Formula weight	480.89
Color	Red
Crystal dimensions (mm)	0.18 × 0.14 × 0.03
Temperature (K)	110
Wavelength (Å)	0.71070
Crystal system	Monoclinic
Space group	$P2_1/c$
Unit cell dimensions (Å, °)	a = 11.501(7)
	b = 10.417(7)
	c = 17.149(11)
	α = 90
	β = 93.344(3)
	γ = 90
Volume (Å^3)	2051(2)
Z	4
Calculated density (g cm^{-3})	1.609
Absorption coefficient (mm^{-1})	1.197
F(000)	1016
Theta range for data collection (°)	3.0–27.5
Absorption correction	Lorentz-polarization
Refinement method	Full-matrix least squares on F^2
No. of reflections measured	Total: 15511, unique: 4654
Data/restraints/parameters	3991/0/279
Goodness-of-fit on F^2	0.969
R indices [$I > 2\sigma(I)$]	R_1 = 0.1000, wR_2 = 0.2659
$\Delta\rho_{max}$, $\Delta\rho_{min}$ (e Å^3)	3.71, −1.56

DNA cleavage experiments were carried out according to reported procedure [46]. For the gel electrophoresis experiment, supercoiled pBR322 DNA was treated with the cobalt(III) complexes in TEA buffer (10 mmol Tris acetate, 10 mmol EDTA, pH 8.0) and the solution was then incubated at 37 °C for 2 h. Loaded 20 μL of DNA sample (mixed with bromophenol blue dye, 1:1 ratio), carefully into the wells, along with standard DNA marker. The samples were analyzed by electrophoresis for 30 min at 50 V on a 0.8% agarose gel in TEA (4.84 g Tris–acetate, 0.5 mol EDTA/1 L, pH 8.0). The gel was stained with 10 μg/mL ethidium bromide and observes the bands under illuminator.

2.7. Protein binding studies

The excitation wavelength of BSA at 280 nm and the emission at 344 nm were monitored for the protein binding studies. The excitation and emission slit widths and scan rates were maintained constant for all of the experiments. A stock solution of BSA was prepared in 5 mM Tris–HCl/50 mM NaCl buffer (pH = 7.2) and stored in the dark at 4 °C for further use. A concentrated stock solution of the compounds was prepared as mentioned for the DNA binding experiments, except that the phosphate buffer was used instead of a Tris–HCl buffer for all of the experiments. Titrations were manually done by using a micropipet for the addition of the complexes.

2.8. Antioxidant assays

2.8.1. DPPH· scavenging assay

The 2,2-diphenyl-1-picrylhydrazyl (DPPH) radical scavenging activity of the compounds was measured according to the method of Blois [47]. The DPPH radical is a stable free radical. Because of the odd electron, DPPH shows a strong absorption band at 517 nm in the visible spectrum. As this electron becomes paired off in the presence of a free radical scavenger, the absorption vanishes and the resulting decolorization is stoichiometric with respect to the number of electrons taken up. Various concentrations of the experimental complexes were taken and the volume was

adjusted to 100 μL with methanol. About 5 mL of a 0.1 mM methanolic solution of DPPH was added to the aliquots of samples and standards (BHT and vitamin C) and shaken vigorously. A negative control was prepared by adding 100 μL of methanol in 5 mL of 0.1 mM methanolic solution of DPPH. The tubes were allowed to stand for 20 min at 27 °C. The absorbance of the sample was measured at 517 nm against the blank (methanol).

2.8.2. OH· scavenging assay

The hydroxyl radical scavenging activity of the compounds has been investigated by using the Nash method [48]. *In vitro* hydroxyl radicals were generated by an Fe^{3+}/ascorbic acid system. The detection of hydroxyl radicals was carried out by measuring the amount of formaldehyde formed from the oxidation reaction with DMSO. The formaldehyde produced was detected spectrophotometrically at 412 nm. A mixture of 1.0 mL of iron-EDTA solution (0.13% ferrous ammonium sulfate and 0.26% EDTA), 0.5 mL of EDTA solution (0.018%), and 1.0 mL of DMSO (0.85% DMSO (v/v) in 0.1 M phosphate buffer, pH 7.4) were sequentially added in the test tubes. The reaction was initiated by adding 0.5 mL of ascorbic acid (0.22%) and was incubated at 80–90 °C for 15 min in a water bath. After incubation, the reaction was terminated by the addition of 1.0 mL of ice-cold trichloroacetic acid (17.5% w/v). Subsequently, 3.0 mL of Nash reagent was added to each tube and left at room temperature for 15 min. The intensity of the color formed was measured spectrophotometrically at 412 nm against the reagent blank.

2.8.3. NO· scavenging assay

The assay of nitric oxide (NO) scavenging activity is based on a method [49] where sodium nitroprusside in aqueous solution at physiological pH spontaneously generates nitric oxide, which interacts with oxygen to produce nitrite ions. These can be estimated using the Greiss reagent. Scavengers of nitric oxide compete with oxygen leading to less production of nitrite ions. For the experiment, sodium nitroprusside (10 mM) in phosphate buffered saline was mixed with a fixed concentration of the complex and standards were incubated at room temperature for 150 min. After the incubation period, 0.5 mL of Griess reagent containing 1% sulfanilamide, 2% H_3PO_4 and 0.1% *N*-(1-naphthyl) ethylenediamine dihydrochloride were added. The absorbance of the chromophore formed was measured at 546 nm.

2.9. In vitro cytotoxic activity evaluation by MTT assays

Standard 3-(4,5-dimethylthiozole)-2,5-diphenyltetraazolium bromide (MTT) assay procedures were used [50]. The monolayer cells were detached with trypsin–ethylenediaminetetraacetic acid (EDTA) to make single cell suspensions and viable cells were counted using a hemocytometer and diluted with medium containing 5% FBS to give final density of 1×10^5 cells/mL. One hundred microliters per well of cell suspension were seeded into 96-well plates at plating density of 10,000 cells/well and incubated to allow for cell attachment at 37 °C, 5% CO_2, 95% air and 100% relative humidity. After 24 h the cells were treated with serial concentrations of the test samples. They were initially dissolved in neat dimethylsulfoxide (DMSO) to prepare the stock (200 mM) and stored frozen prior to use. At the time of drug addition, the frozen concentrate was thawed and an aliquot was diluted to twice the desired final maximum test concentration with serum free medium. Additional three, 10 fold serial dilutions were made to provide a total of four drug concentrations. Aliquots of 100 μL of these different drug dilutions were added to the appropriate wells already containing 100 μL of medium, resulted the required final drug concentrations. Following drug addition the plates were incubated for an additional 48 h at 37 °C, 5% CO_2, 95% air and 100% relative humidity. The medium containing without samples were served as control and triplicate were maintained for all concentrations.

MTT is a yellow water soluble tetrazolium salt. A mitochondrial enzyme in living cells, succinate-dehydrogenase, cleaves the tetrazolium ring, converting the MTT to an insoluble purple formazan. Therefore, the amount of formazan produced is directly proportional to the number of viable cells. After 48 h of incubation, 15 μL of MTT (5 mg/mL) in phosphate buffered saline (PBS) was added to each well and incubated at 37 °C for 4 h. The medium with MTT was then flicked off and the formed formazan crystals were solubilized in 100 μL of DMSO and then measured the absorbance at 570 nm using a micro-plate reader. The% cell inhibition was determined using the following formula. % Cell inhibition = 100 − Abs (sample)/Abs (control) × 100. Nonlinear regression graph was plotted between % cell inhibition and $\log_{10}$ concentration and IC_{50} was determined using GraphPad Prism software.

3. Results and discussion

The analytical data of the ligands and their corresponding complexes summarized in the experimental section agreed well with the theoretical values within the limit of experimental error and confirmed the general formulae $[Co(L^n)_2]Cl$ (n = 1–3) proposed for the new complexes. All these complexes are stable in air at room temperature and highly soluble in common organic solvents and water. In addition, ESI-Mass spectra of **1**, **2** and **3** were also confirmed the molecular weight (496.88, 524.94 and 649.08) of the complexes. The molecular ion peaks (445.2, 473.4 and 597.2) $[M-Cl]^+$ were in good agreement with the suggested empirical formulae as indicated from elemental analyses.

3.1. X-ray crystallography

The single crystal ORTEP diagram of complex **1** with atom numbering scheme is shown in Fig. 1. Selected bond lengths and bond angles are given in Table 2. The coordination geometry around Co(III) metal ion can be described as a distorted octahedron, the cobalt atom being bonded with two tridentate NNS donor ligand molecules in such a way that four 5-membered chelate rings are

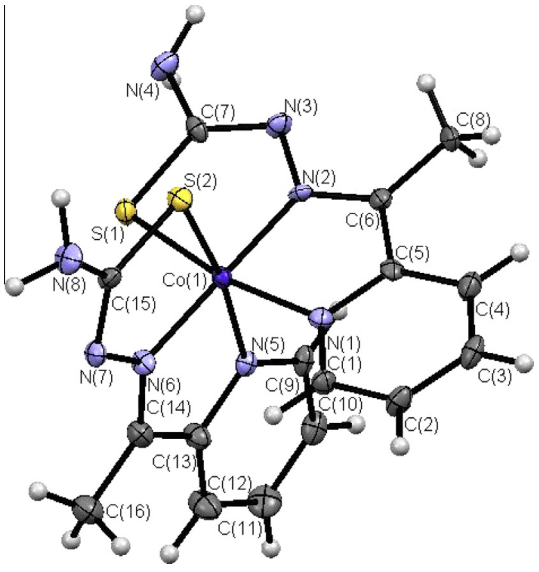

Fig. 1. ORTEP view of complex **1**.

Table 2
Selected bond lengths (Å) and angles (°) for the complex **1.**

Co(1)—S(1)	2.2304(11)	S(1)—Co(1)—S(2)	90.61(4)
Co(1)—S(2)	2.2136(12)	S(1)—Co(1)—N(1)	169.07(10)
Co(1)—N(1)	1.952(3)	S(1)—Co(1)—N(2)	86.23(11)
Co(1)—N(2)	1.888(3)	S(1)—Co(1)—N(5)	91.62(10)
Co(1)—N(5)	1.962(3)	S(1)—Co(1)—N(6)	94.54(12)
Co(1)—N(6)	1.897(3)	S(2)—Co(1)—N(1)	90.00(11)
S(1)—C(7)	1.753(4)	S(2)—Co(1)—N(2)	92.80(12)
S(2)—C(15)	1.754(4)	S(2)—Co(1)—N(5)	169.57(10)
N(1)—C(1)	1.345(5)	S(2)—Co(1)—N(6)	86.93(12)
N(1)—C(5)	1.363(5)	N(1)—Co(1)—N(2)	82.85(14)
N(2)—N(3)	1.382(5)	N(1)—Co(1)—N(5)	89.74(14)
N(2)—C(6)	1.316(5)	N(1)—Co(1)—N(6)	96.39(15)
N(3)—C(7)	1.327(5)	N(2)—Co(1)—N(5)	97.50(15)
N(4)—C(7)	1.341(5)	N(2)—Co(1)—N(6)	179.19(15)
N(5)—C(9)	1.348(5)	N(5)—Co(1)—N(6)	82.74(15)
N(5)—C(13)	1.372(5)		
N(6)—N(7)	1.385(5)		
N(6)—C(14)	1.397(6)		
N(7)—C(15)	1.329(5)		
N(8)—C(15)	1.329(5)		

formed. The azomethinic nitrogens [N(2) and N(6)] are placed in a *trans* position. The chlorine atom acts as a counterion.

The NNS planes of the ligands are practically orthogonals, with angles near to 90°. The bond lengths are similar to those found for other cobalt(III) compounds with pyridine-2-carbaldehyde thiosemicarbazone ligand [28]. In the same way, there are not appreciable differences in the bond lengths with respect to the free thiosemicarbazone ligand [51], except for the N(3)—C(7)/N(7)—C(15) and C(7)—S(1)/C(14)—S(2) distances. In the free ligand, the N(3)—C(7) and C(7)—S bond lengths are 1.314(3) and 1.692(3) Å. The shortening of the N(3)—C(7) length with respect to the free ligand suggests an increase in the double bond character for this bonding under complexation. The C(7)—S bond shows the opposite tendency decreasing in double bond character with respect to the free ligand. In complex **1** the four nitrogen and two sulfur atoms exhibit ligand–metal–ligand bite angles and are found to be S(1)—Co(1)—N(2), 86.23(11); S(2)—Co(1)—N(6), 86.93(12); N(1)—Co(1)—N(2), 82.85(14); N(5)—Co(1)—N(6), 82.74(15) respectively. The trans angles of the complex **1** [S(1)—Co(1)—N(1), 169.07(10); S(2)—Co(1)—N(5), 169.57(10); N(2)—Co(1)—N(6), 179.19(15), respectively] deviate slightly from the expected linear trans geometry. The bond lengths involving the cobalt(III) ion and the links in the thiosemicarbazone chain are close to those found in NNS and ONS systems of alkyl- and arylthiosemicarbazones with cobalt(III) ions [52–55]. The Co—S and Co—N_{azo} distances range between 2.20–2.23 and 1.86–1.96 Å, respectively, in all thiosemicarbazone-cobalt(III) compounds [34,36,38].

3.2. Infrared spectra

The IR spectra of the ligands and their corresponding complexes provided significant information about the metal ligand bonding. The spectra of the ligands displayed characteristic absorption bands at 3241–3183, 1613–1598, 1583–1578 and 836–801 cm^{-1} due to hydrazinic ν_{N-H}, azomethine $\nu_{C=N}$, $\nu_{C=N}$ (pyridine) and $\nu_{C=S}$ vibrations respectively. The bands due to hydrazinic ν_{N-H} and $\nu_{C=S}$ vibrations of the free ligands were absent in the complexes, thus indicating that thioenolisation and deprotonation had taken place prior to coordination. This fact was further confirmed by the appearance of two new bands in the range 1630–1598 cm^{-1} and 773–753 cm^{-1} that corresponds to $\nu_{(C=N-N=C)}$ and $\nu_{(C-S)}$ stretching vibrations respectively [33,35]. The bands attributed to azomethine $\nu_{(C=N)}$ stretching of the ligands were shifted to lower frequencies (1599–1579 cm^{-1}) in the metal complexes indicating the coordination of the ligands to metal through the azomethine nitrogen atom [56]. Further the pyridine ring $\nu_{(C=N)}$ group frequency shifted to lower frequencies 1577–1560 cm^{-1} in the complexes indicating that the coordination of the pyridine nitrogen also. Hence, from the infrared spectroscopic data, it is inferred that the azomethine nitrogen, pyridine nitrogen and sulfur atoms are involved in the coordination to metal ion in all the complexes.

3.3. Electronic spectra

The electronic spectra of the free ligands exhibited two to three bands in the region 341–202 nm corresponding to the intra ligand n–π^* transition of the azomethine portion and π–π^* transitions of the aromatic ring. The bands are shifted to higher energy region in the spectra of complexes and appeared in the region 372–225 nm. In addition an intense absorption band observed in all the complexes in the regions of 420–402 nm were assigned to ligand to metal charge transfer transition [37].

3.4. ^1H NMR Spectra

The ^1H NMR spectra of free ligands showed a signal at δ 10.65–10.31 ppm, characteristics of hydrazinic NH proton [42]. But, the NMR spectra of complexes **1**–**3** did not register any signals corresponding to hydrazinic NH proton. This indicated that the ligands adopted the thioenol form, followed by deprotonation prior to coordination with the metal ion. The signals corresponding to the protons of aromatic moieties of the ligands and their complexes were observed as multiplets in the range of δ 8.68–7.21 ppm. The peak appeared at 3.08–2.20 ppm has been assigned to methyl group [42,57]. In addition, —NH—R proton appeared in the region at 10.25–8.10 ppm [57].

Based on the analytical, spectroscopic characterization (FT-IR, UV-visible, ^1H NMR and ESI-Mass) and single-crystal X-ray crystallographic studies of complex **1**, an octahedral structure has been proposed for all the new cobalt(III) complexes (Scheme 1).

3.5. DNA binding properties

3.5.1. Fluorescence spectral studies

Luminescence measurement was performed to clarify the binding affinity of cobalt complexes to the CT-DNA. The results of the fluorescence titration for complexes **1**–**3** with CT-DNA are illustrated in Fig. 2. Complexes bound to DNA through intercalation often show decreased intensities (hypochromism) and a red shift of their emission bands due to the strong stacking interaction between the aromatic chromophores of the complex and base pairs of DNA [58]. All these complexes could emit luminescence at ambient temperature with a maximum excitation wavelength at 400 and emission wavelength at 429 nm containing Tris–HCl buffer (5 mM Tris–HCl/50 mM NaCl buffer for pH = 7.2). Upon increasing concentration of CT-DNA the emission intensities of complex **1** exhibited hypochromism of 21% with red shift of 1 nm at 430 nm respectively. However the emissive bands at 429 nm exhibited hypochromism up to 20.8% and 20% of the initial fluorescence intensity for complexes **2** and **3**. Based on the emission behavior of these DNA binding enhancement, the effect of intensity of bands decreased from the original intensities. The intrinsic binding constants were obtained according to the following Scatchard equation.

$$C_F = C_T[(I/I_0) - P]/[1 - P]$$

where C_T is concentration of the probe (complex) added, C_F is the concentration of the free probe, and I_0 and I are its emission intensities in the absence and in the presence of DNA, respectively. P is the ratio of the observed emission quantum yield of the bound probe to the free probe. The value of P was obtained from a plot

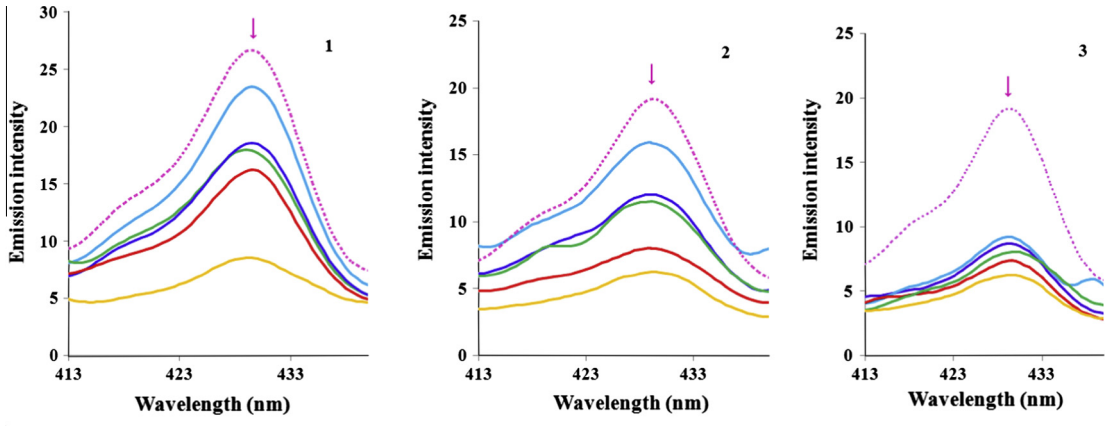

Fig. 2. Flourescence spectra of cobalt(III) complexes **1**–**3** in 5 mM Tris-HCl/50 mM NaCl buffer at pH 7.2 and arrows an indicate absence and presence of incresing amounts of CT-DNA concentration at 25 °C. [Complex = 25 μM (—— lines)], DNA = 0–25 μM.

of I/I_0 versus 1/[DNA] such that the limiting emission yield is given by the *y*-Intercept. The amount of bound probe (C_B) at any concentration was equal to $C_T - C_F$. The Scatchard plots of r/C_f versus r for complexes **1**–**3** with increasing concentration of CT-DNA shown in Fig. 3. A plot of r/C_F versus r (=C_B/[DNA]) gave the binding isotherm and the best fit of the data resulted in the intrinsic binding constant (K_b) values was calculated from the ratio of slope and the intercept [59]. It has been found that the binding constant (K_b) for complexes **1**, **2** & **3** were 1.2×10^5 M^{-1}, 8.27×10^4 M^{-1} & 9.4×10^5 M^{-1} respectively. The observed values of K_b revealed that the complexes bind to DNA via the intercalative mode [60]. From the results obtained, it has been found that complex **3** strongly bound with CT-DNA than other two complexes and the order of binding affinity is **3** > **1** > **2**. Even though the binding mode of the complexes needs to be discussed furthermore experiments.

3.5.2. Competitive binding with methylene blue

The emission titration results indicate that the complexes effectively bind to DNA. In order to confirm the binding mode and compare their binding affinities, methylene blue (MB) displacement experiments were carried out. Methylene Blue (MB) is a planar cationic dye which is widely used as a sensitive fluorescence probe for native DNA. MB emits intense fluorescent light in the presence of DNA due to its strong intercalation between the adjacent DNA base pairs. The displacement technique is based on the decrease of fluorescence resulting from the displacement of MB from a DNA sequence by a quencher, and the quenching is due to the reduction of the number of binding sites on the DNA that are available to the MB. The fluorescence quenching spectra of DNA-bound MB for complexes **1**, **2** and **3** were shown in Fig. 4. This illustrate that, as the concentration of the complexes increases, the emission band at 684 nm exhibited hypochromism up to 16.25%, 43.40% and 29.90% of the initial fluorescence intensity. The observed decrease in the fluorescence intensity clearly indicates that the MB molecules are displaced from their DNA binding sites and are replaced by the complexes under investigation [61]. Quenching data were analyzed according to the following Stern–Volmer equation:

$$F^0/F = K_q[Q] + 1$$

where F^0 is the emission intensity in the absence of compound, F is the emission intensity in the presence of compound, K_q is the quenching constant, and [Q] is the concentration of the compound. The K_q value is obtained as a slope from the plot of F_0/F versus [Q]. In the Stern–Volmer plot (Fig. 5) of F^0/F versus [Q], the quenching constant (K_q) is obtained from the slope which was 7.16×10^3 M^{-1}, 4.82×10^3 M^{-1} and 1.04×10^4 M^{-1} for the complexes **1**, **2** and **3**, respectively. Further the apparent DNA binding constant (K_{app}) were calculated using the following equation,

$$K_{MB}\ [MB] = K_{app}\ [complex]$$

(where the complex concentration has the value at a 50% reduction of the fluorescence intensity of MB, K_{MB} (1.0×10^{-7} M^{-1}) is the DNA binding constant of MB to DNA, [MB] = 7.5 μM), where found to be 5.37×10^5 M^{-1}, 3.61×10^5 M^{-1} and 7.5×10^5 M^{-1} respectively for **1**, **2** and **3**. The experimental results data again suggest that the complexes bind to DNA via intercalation but the complex **3** binds to DNA more strongly than the complexes **1** and **2**, which is in agreement with the results observed from the emission spectra. Since these changes indicate only one kind of quenching process, it may be concluded that all of the complexes can bind to DNA via the same mode.

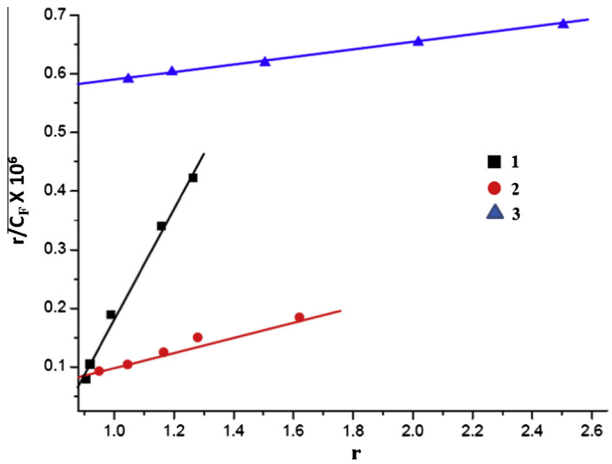

Fig. 3. Scatchard plots of r/C_f versus r for complexes **1**–**3** with incresing concentration of CT-DNA.

3.6. DNA cleavage activity

The ability of the metal complexes to perform DNA cleavage is generally monitored by agarose gel electrophoresis and in the present work pBR322 DNA was chosen to investigate its cleavage. The DNA cleavage was controlled by relaxation of the supercoiled circular form of CT-DNA into the open circular form and linear form. When circular plasmid DNA is run on horizontal gel using electrophoresis, the supercoiled form will migrate first (Form I).

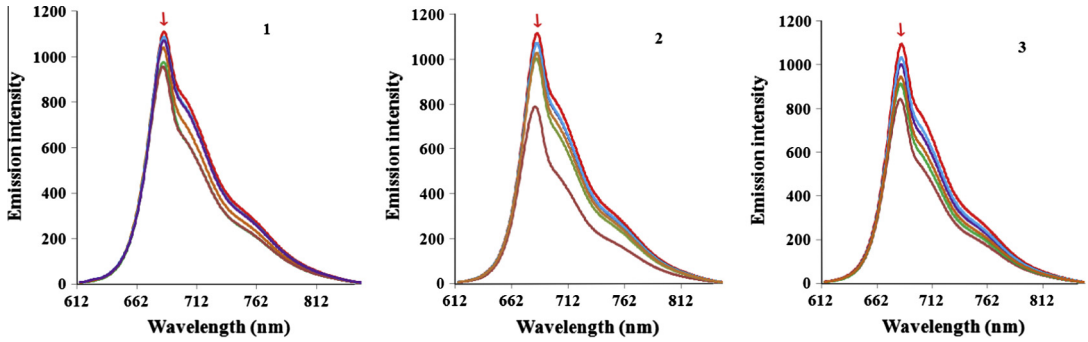

Fig. 4. Flourescence quenching curves of MB bound to CT-DNA in presence of complexes (**1**–**3**) in 5 mM Tris–HCl/50 mM NaCl buffer at pH 7.2. Arrow shows an indicate emission intensity changes upon incresing concentration of complexes at 25 °C. [DNA = 7.5 μM], [MB] = 7.5 μM and complexes [0–50 μM].

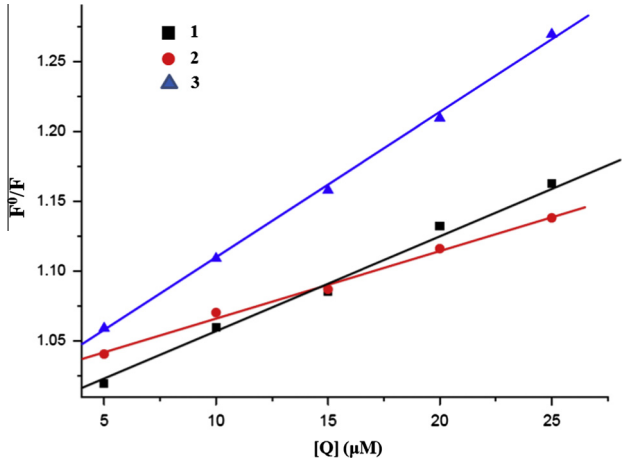

Fig. 5. Stern–Volmer plots of the MB–DNA fluorescence titration for complexes **1**–**3**.

If the strands (nicking) of the selected DNA is cleaved by interaction with the metal complexes, the supercoils will relax to produce an open circular form (Form II) that moves slower than form I, whereas with cleavage of both strands to a linear form (Form III) the resulting system will migrate in between the above two forms. As seen in Fig. 6, control photoreactions with control DNA (lane C), resulted in no obvious DNA cleavage was observed. In contrast, photoreactions at 365 nm (lanes 1–6), resulted in significant production of nicked DNA depending on the concentrations of complexes used. As increasing concentrations of complexes **1** and **3**, the amount of Form I (supercoiled form) of pBR322 DNA diminishes gradually, whereas that of Form II (circular form) increases. When concentration reached 40 μg/mL for complex **1**, DNA was completely converted from Form I to Form II. The results indicated

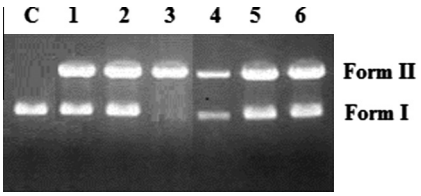

Fig. 6. Agarose gel electrophoresis diagram showing the cleavage of pBR322 DNA by Co(III) Schiff base complex in TAE Buffer (4.84 g Tris base, pH = 8, 0.5 M EDTA/1 L). Lane C, Control DNA (untreated complex); Lanes 1–3, in the different concentrations of complex **1**: (1) 10; (2) 20; (3) 40 μg/mL; Lanes 4–6, in the different concentrations of complex **3**: (1) 10; (2) 20; (3) 40 μg/mL.

that the complex **1** exhibits more effective DNA cleavage activity than the complex **3**.

3.7. Fluorescence quenching of BSA with cobalt(III) complexes

Generally, the fluorescence of BSA is caused by two intrinsic characteristics of the protein, namely tryptophan and tyrosine. Changes in the emission spectra of tryptophan are common in response to protein conformational transitions, subunit associations, substrate binding, or denaturation. Therefore, the intrinsic fluorescence of BSA can provide considerable information on their structure and dynamics and is often utilized in the study of protein folding and association reactions. The interaction of BSA with cobalt complexes was studied by fluorescence measurement at room temperature. A solution of BSA (1 μM) was titrated with various concentrations of the complexes (0–50 μM). Fluorescence spectra were recorded in the range of 290–450 nm upon excitation at 280 nm. The effects of the compound on the fluorescence emission spectrum of BSA are shown in Fig. 7.

The addition of the above complexes to the solution of BSA resulted in a significant decrease of the fluorescence intensity of BSA at 344 nm, up to 43.7%, 43.8% and 97.6% from the initial fluorescence intensity of BSA accompanied by a hypsochromic shift of 2, 2 and 4 nm for complexes **1**, **2** and **3**, respectively. The observed blue shift is mainly due to the fact that the active site in protein is buried in a hydrophobic environment. This result suggested a definite interaction of all of the complexes with the BSA protein [62,63].

Furthermore fluorescence quenching data were analyzed with the Stern–Volmer equation and Scatchard equation. From the plot of I_0/I versus [Q] The quenching constant (K_q) can be calculated using the plot of I_0/I versus [Q] (Fig. 8A). If it is assumed that the binding of compounds with BSA occurs at equilibrium, the equilibrium binding constant can be analyzed according to the Scatchard equation:

$$\log[(I_0 - I)/I] = \log K_{bin} + n \log[Q]$$

where K_{bin} is the binding constant of the compound with BSA and n is the number of binding sites. The number of binding sites (n) and the binding constant (K_{bin}) have been found from the plot of log $(I_0 - I)/I$ versus log [Q] (Fig. 8B). The calculated K_q, K_{bin}, and n values are given in Table 3. The given value of n is around two for all of the compounds, indicating the two binding site of BSA hydrophobic environment. The ability of complexes to quench the emission intensity of BSA, as attributed from K_q and K_{bin} values. Among the three complexes, the complex **3** has better interaction with BSA than the other two complexes. The order of efficiency of the tested complexes to bind with BSA was observed as **3** > **1** > **2**.

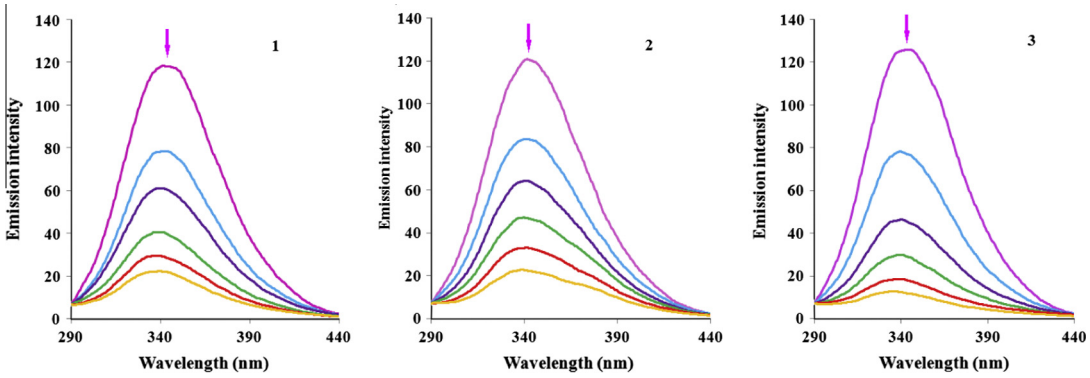

Fig. 7. The emission spectrum of bovine serum albumin (BSA) (1 μM; λ_{ex} = 280 nm, λ_{em} = 344 nm) in the presence of increasing amounts of the complexes **1–3** (0–50 μM). The arrow shows that the emission intensity decreases upon the increase in concentration of the compounds.

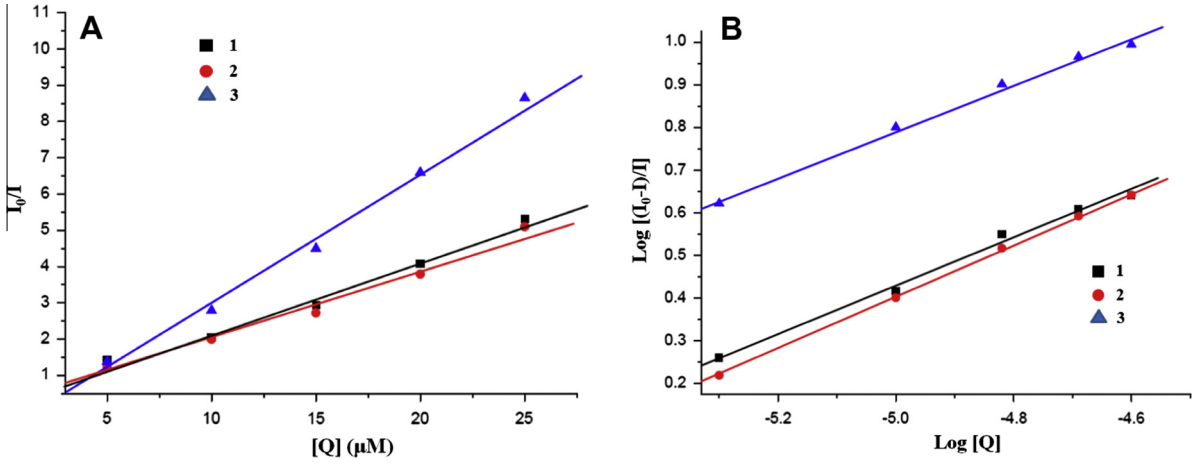

Fig. 8. Stern–Volmer plots (A) and Scatchard plots (B) of the fluorescence titration of the complexes **1–3** with BSA.

Table 3
Quenching constant (K_q), binding constant (K_{bin}), and number of binding sites (n) for the interactions of complexes with BSA.

Complex	K_q (M^{-1})	K_{bin} (M^{-1})	N
1	1.96×10^5	2.38×10^5	1.83
2	1.90×10^5	2.27×10^5	1.85
3	3.66×10^5	5.61×10^5	2.02

Table 4
Antioxidant activity of ligands, cobalt(III) complexes, BHT and vitamin C against various radicals.

Compound	IC_{50} (μM)		
	DPPH	OH	NO
HL^1	63.03 ± 0.2	58.39 ± 0.3	38.23 ± 0.2
HL^2	53.45 ± 0.3	52.00 ± 0.1	36.52 ± 0.5
HL^3	65.56 ± 0.2	70.03 ± 0.4	43.06 ± 0.3
1	15.43 ± 0.4	35.96 ± 0.2	36.85 ± 0.1
2	14.44 ± 0.1	31.86 ± 0.3	32.80 ± 0.3
3	16.53 ± 0.3	39.19 ± 0.3	40.39 ± 0.3
BHT	86.53 ± 0.6	163.80 ± 0.5	154.30 ± 0.8
Vitamin C	147.20 ± 0.8	232.20 ± 0.7	215.72 ± 0.9

3.8. Evaluation of radical scavenging ability

Free radicals play an important role in inflammatory process. Thus, the compounds with possible antioxidant properties could play a crucial role against the inflammation and lead to potentially effective drugs. Antioxidants that exhibit radical scavenging activity are receiving increased attention since they present interesting anticancer, anti-ageing and anti-inflammatory activities [64–66]. Therefore, the compounds with antioxidant properties may offer protection against rheumatoid arthritis and inflammation.

The radical scavenging activities of our compounds along with standards, such as butylated hydroxyl toluene (BHT) and Vitamin C in a cell free system, have been examined with reference to DPPH radicals (DPPH·), hydroxyl radicals (OH·), and nitric oxide (NO), and their corresponding IC_{50} values were shown in Table 4. From Table 4, it can be concluded that a much less scavenging activity

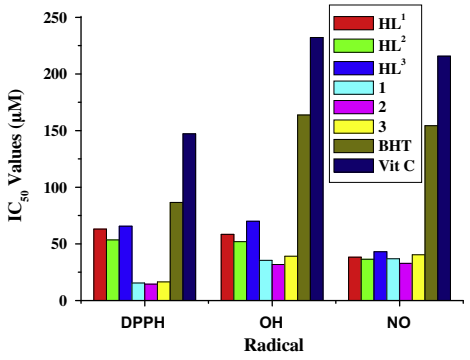

Fig. 9. Radical scavenging activity of the compounds (HL^{1-3} & **1–3**) and the standards, BHT and Vitamin C.

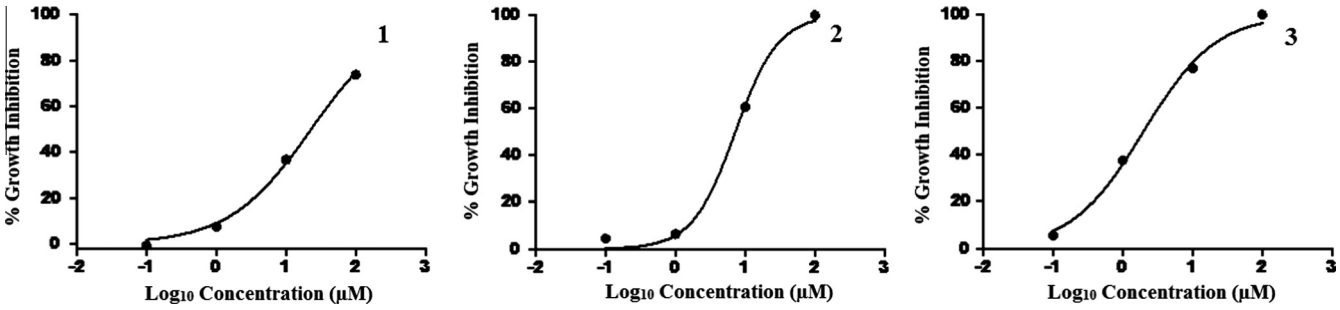

Fig. 10a. The % growth inhibition against $\log_{10}$ concentrations of cobalt(III) complexes (**1**–**3**) on breast cancer cell line (MCF-7).

was exhibited by the free ligands when compared to that of their corresponding cobalt complexes which is due to the chelation of them with the cobalt ions. The overall scavenging activity of the tested compounds was found to increase in the order of HL^3 < HL^1 < HL^2 < **3** < **1** < **2** (Fig. 9). The complex **2** showed better activity compared to the other complexes, which may be due to the electron donating effect of methyl group present in HL^2 ligand. The IC_{50} values (Table 4) indicated that the various radical scavenging activities of the complexes are in the order of $NO^{\cdot}$ < $OH^{\cdot}$ < $DPPH^{\cdot}$. The lower IC_{50} values observed in antioxidant assays have demonstrated that these complexes have a strong potential to be applied as scavengers to eliminate the radicals. Further, it is significant to mention that the metal complexes synthesized herein possess superior antioxidant activity against the above said radicals than that of the standard antioxidant butylated hydroxyl toluene (BHT) and Vitamin C.

3.9. Cytotoxic activity evaluation by MTT assay

Since the DNA binding and antioxidant experiments conducted so far revealed that the cobalt(III) complexes exhibit good binding and antioxidant activity, it is considered worthwhile to study the cytotoxic activity of these complexes. Cytotoxicity is a common

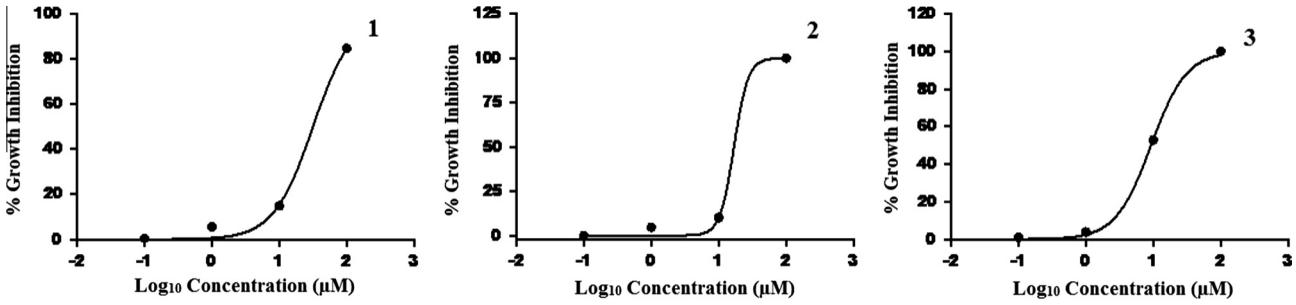

Fig. 10b. The % growth inhibition against $\log_{10}$ concentrations of cobalt(III) complexes (**1**–**3**) on skin carcinoma cell line (A431).

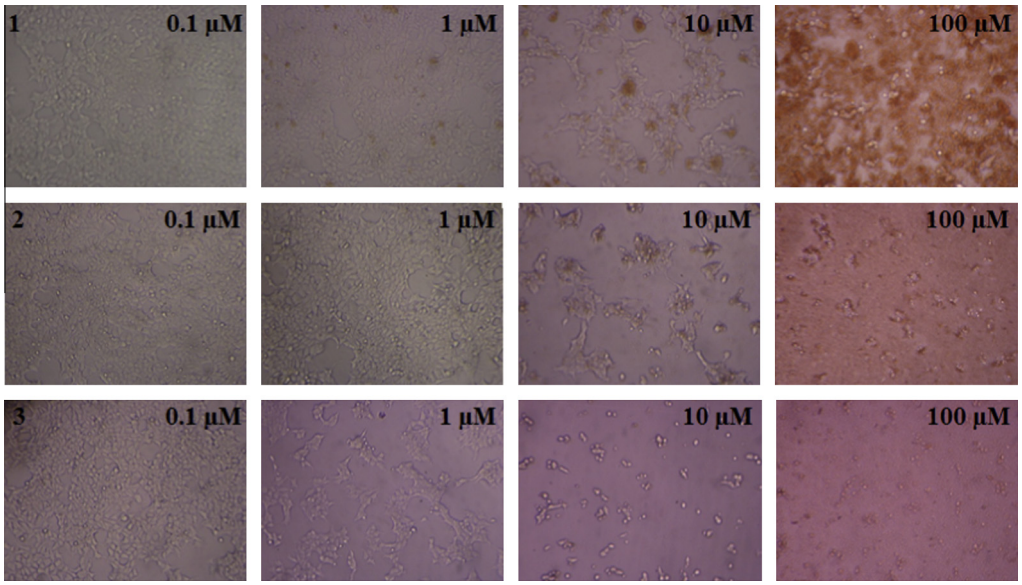

Fig. 11a. Cytotoxic effect of cobalt(III) complexes against MCF-7 at different concentrations (0.1 μM, 1.0 μM, 10 μM, 100 μM). Cell viability decreased with increasing concentrations of complexes.

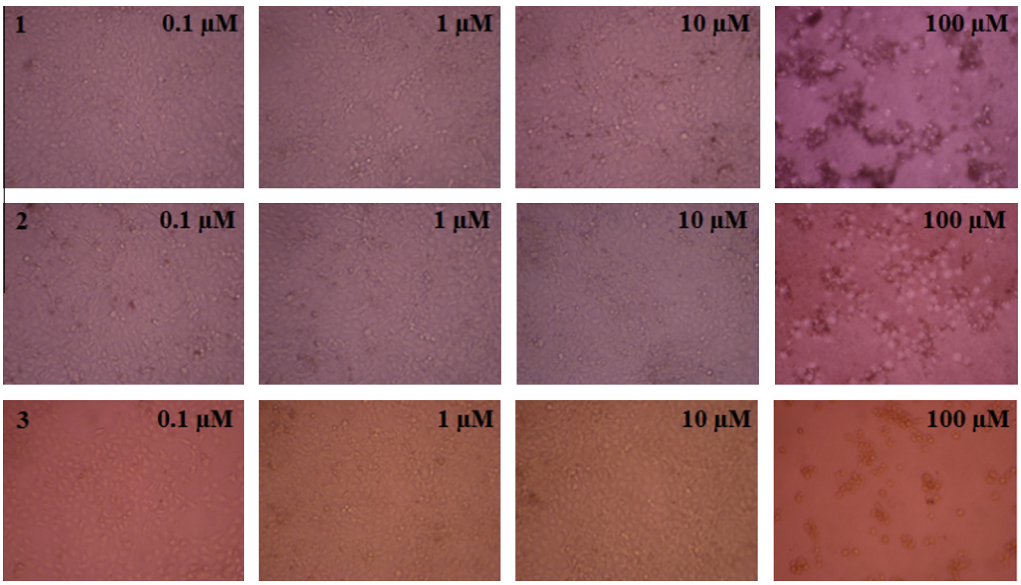

Fig. 11b. Cytotoxic effect of cobalt(III) complexes against A431 at different concentrations (0.1 μM, 1.0 μM, 10 μM, 100 μM). Cell viability decreased with increasing concentrations of complexes.

limitation in terms of the introduction of new compounds in the pharmaceutical industry.

Cytotoxic potential of newly synthesized cobalt(III) complex was investigated on two cell lines including human skin carcinoma cell line (A431) and human breast cancer cell line (MCF-7). The compounds were applied in range of concentrations from 0.1 to 100 μM and cells left for 48 h. The activities of the compounds were determined by means of a colorimetric assay (MTT assay) which measures mitochondrial dehydrogenase activity as an indication of cell viability, and the results were expressed in terms of IC_{50} values. Upon increasing the concentration of complexes from 0.1 μM to 100 μM, the % cell inhibition also increased. It is evident from Figs. 10 and 11 that the number of cells decreased with an increase in the concentration of the complexes. All the complexes have cytotoxic potencies, with IC_{50} values generally in the low micromolar range. The IC_{50} values of complexes and standard are given in Table 5. As a general observation, complex **3** is more active than the other complexes in the cell lines tested, and it exhibited much better activity than cisplatin in the MCF-7 cell line. The cytotoxicity of the tested complexes against both cancer cell lines follows the order **3** > **2** > **1**. The higher cytotoxic activity for the complex **3** may be due to terminal phenyl substitution of the coordinated HL^3 ligand. By comparing the cytotoxicity with that of the conventional standard cisplatin, we found that the complexes exhibited excellent activity in both the cancer cell lines. However, among the tested cell lines, the cytotoxic activity of complexes against human breast cancer cell line (MCF-7) was higher than that of skin carcinoma cell line (A431).

Table 5
IC_{50} (μM) value of cobalt(III) complexes and cisplatin against human breast cancer cell line (MCF-7) and skin carcinoma cell line (A431).

Complex	IC_{50} (μM)[a]	
	MCF-7	A431
1	22.99 ± 0.08	32.12 ± 1.03
2	7.24 ± 0.09	16.85 ± 2.09
3	1.99 ± 0.13	9.30 ± 0.03
Cisplatin	3.19 ± 0.02	12.33 ± 0.07

[a] Fifty percent inhibitory concentration after exposure for 48 h in the MTT assay.

4. Conclusions

2-Acetylpyridine N-substituted thiosemicarbazone ligands and their corresponding cobalt(III) complexes have been synthesised and characterized. The molecular structure of the complex **1** has been determined by single crystal X-ray diffraction study and it showed that cobalt(III) cation is coordinated with two ligand molecules. The two ligand molecules in this complex are deprotonated at the imino nitrogen, resulting in two tridendate monoanionic species coordinating to the central metal via the thiolato sulfur, imine nitrogen and pyridine nitrogen, resulting in a distorted octahedral moiety. The DNA binding properties of the complexes were investigated by fluorescence measurements. The results supported the fact that the complexes bind to CT-DNA via intercalation. The binding constant values (K_b) showed that the DNA binding affinity increased in the order **3** > **1** > **2**. The protein binding properties of the complexes examined by the fluorescence spectra suggested that the binding affinity of the complex **3** was stronger than that of the other complexes. In addition, the complex **1** can efficiently cleave the pBR322 DNA. The antioxidant studies revealed that all the complexes exhibited higher activities compared to the standards BHT and vitamin C. The complexes **1**–**3** exhibited good cytotoxic activity against MCF-7 and A431 cancer cell line. In particular, among the three complexes, complex **3** exhibited higher cytotoxicity against above cancer cell lines and the IC_{50} value of the complexes showed that the activity is higher than that of cisplatin.

Acknowledgements

We are thankful to the IISC Bangalore, STIC Cochin, SAIF Panjab University, Chandigarh, KMCH Coimbatore and Biogenics Hubli, India for providing instrumental facilities. The author (R.N) thankful to DST for financial assistant in the form Project (No. SR/FT/CS-95/2010).

Appendix A. Supplementary material

CCDC 917524 contains the supplementary crystallographic data for the complex $[Co(L^1)_2]Cl$. These data can be obtained free of charge via http://www.ccdc.cam.ac.uk/conts/retrieving.html, or

from the Cambridge Crystallographic Data Centre, 12 Union Road, Cambridge CB2 1EZ, UK; fax: (+44) 1223-336-033; or e-mail: deposit@ccdc.cam.ac.uk. Supplementary data associated with this article can be found, in the online version, at http://dx.doi.org/10.1016/j.jphotobiol.2013.11.008.

References

[1] B. Lippert, Cisplatin: Chemistry and Biochemistry of a Leading Anticancer Drug, Wiley Interscience, 1999.
[2] A.S. Abu-Surrah, M. Kettunen, Platinum group antitumor chemistry: design and development of new anticancer drugs complementary to cisplatin, Curr. Med. Chem. 13 (2006) 1337–1357.
[3] C.S. Allardyce, P.J. Dyson, Ruthenium in medicine: current clinical uses and future prospects, Platinum Met. Rev. 45 (2001) 62–69.
[4] I. Ott, R. Gust, Non platinum metal complexes as anti-cancer drugs, Arch. Pharm. Chem. Life 340 (2007) 117–126.
[5] M.A. Jakupec, M. Galanski, V.B. Arion, C.G. Hartinger, B.K. Keppler, Antitumer metal compounds: more than theme and variations, Dalton Trans. (2008) 183–194.
[6] P. Yang, M. Guo, Interactions of organometallic anticancer agents with nucleotides and DNA, Coord. Chem. Rev. 185 (1999) 189–211.
[7] S.K. Hadjikakou, N. Hadjiliadis, Antiproliferative and anti-tumor activity of organotin compounds, Coord. Chem. Rev. 253 (2009) 235–249.
[8] K. Strohfeldt, M. Tacke, Bioorganometallic fulvene-derived titanocene anticancer drugs, Chem. Soc. Rev. 37 (2008) 1174–1187.
[9] D.K. Demertzi, A. Domopoulou, M.A. Demertzis, A. Papageorgiou, D.X. West, Palladium(I1) complexes of 2-acetylpyridine N(4)-propyl, N(4)-dipropyl and 3-Hexa methyleneiminylthiosemicarbazones with potentially interesting biological activity, synthesis, spectral properties, antifungal and *in vitro* antitumor activity, Polyhedron 16 (1997) 3625–3633.
[10] P.M. Abeysinghe, M.M. Harding, Antitumour bis(cyclopentadienyl) metal complexes: titanocene and molybdocene dichloride and derivatives, Dalton Trans. 32 (2007) 3474–3482.
[11] Y.J. Zheng, X.W. Li, Y.T. Li, Z.Y. Wub, C.W. Yan, Synthesis and structure of new tetracopper(II) complexes bridged by 2-{N0-[2-(dimethylamino)ethyl] oxamido} benzoate: DNA-binding and anticancer activity, J. Photochem. Photobiol., B 114 (2012) 27–37.
[12] X.W. Li, X.J. Li, Y.T. Li, Z.Y. Wua, C.W. Yan, Syntheses and structures of new trimetallic complexes bridged by N-(5-chloro-2-hydroxyphenyl)-N′-[3-(dimethylamino) propyl]oxamide: Cytotoxic activities, and reactivities towards DNA and protein, J. Photochem. Photobiol., B 118 (2013) 22–32.
[13] C.G. Hartinger, P.J. Dyson, Bioorganometallic chemistry from teaching paradigms to medicinal applications, Chem. Soc. Rev. 38 (2009) 391–401.
[14] A.D. Richards, A. Rodger, Synthetic metallomolecules as agents for the control of DNA structure, Chem. Soc. Rev. 36 (2007) 471–483.
[15] A. Terron, J.J. Fiol, A. García-Raso, M. Barceló-Oliver, V. Moreno, Biological recognition patterns implicated by the formation and stability of ternary metal ion complexes of low- molecular-weight formed with amino acid/peptides and nucleobases/nucleosides, Coord. Chem. Rev. 251 (2007) 1973–1986.
[16] F.R. Keene, J.A. Smith, J.G. Collins, Metal complexes as structure-selective binding agents for nucleic acids, Coord. Chem. Rev. 253 (2009) 2021–2035.
[17] B.M. Zeglis, V.C. Pierre, J.K. Barton, Metallo-intercalators and metallo-insertors, Chem. Commun. 44 (2007) 4565–4579.
[18] F. Arjmand, A. Jamsheera, D.K. Mohapatra, Synthesis, characterization and in vitro DNA binding and cleavage studies of Cu(II)/Zn(II) dipeptide complexes, J. Photochem. Photobiol., B 121 (2013) 75–85.
[19] Z. Travnicek, A. Klanicova, I. Popa, J. Rolcik, Synthetic, spectral, magnetic and in vitro cytotoxic activity studies of cobalt(II) complexes with cytokinin derivatives: X-ray structure of 6-(3-methoxybenzylamino)purinium chloride monohydrate, J. Inorg. Biochem. 99 (2005) 776–786.
[20] R. Senthil Kumar, S. Arunachalam, V.S. Periasamy, C.P. Preethy, A. Riyasdeen, M.A. Akbarsha, Synthesis, DNA binding and antitumor activities of some novel polymer–cobalt(III) complexes containing 1,10-phenanthroline ligand, Polyhedron 27 (2008) 1111–1120.
[21] E. Ramachandran, S.P. Thomas, P. Poornima, P. Kalaivani, R. Prabhakaran, V. Vijaya, V. Vijaya Padma, K. Natarajan, Evaluation of DNA binding, antioxidant and cytotoxic activity of mononuclear Co(III) complexes of 2-oxo-1,2-dihydrobenzo[h]quinoline-3-carbaldehyde thiosemicarbazones, Eur. J. Med. Chem. 50 (2012) 405–415.
[22] R. Eshkourfu, B. Cobeljic, M. Vujcic, I. Turel, A. Pevec, K. Sepcic, M. Zec, S. Radulovic, T. Srdic-Radic, D. Mitic, K. Andjelkovic, D. Sladic, Synthesis, characterization, cytotoxic activity and DNA binding properties of the novel dinuclear cobalt(III) complex with the condensation product of 2-acetylpyridine and malonic acid dihydrazide, J. Inorg. Biochem. 105 (2011) 1196–1203.
[23] L. Gurley, N. Beloukhina, K. Boudreau, A. Klegeris, W.S. Mcneil, The synthesis and characterization of a series of cobalt(II) β-ketoaminato complexes and their cytotoxic activity towards human tumor cell lines, J. Inorg. Biochem. 105 (2011) 858–866.
[24] S.B. Kumar, Z. Mahendrasinh, S. Ankita, R. Mohammedayaz, P. Pragna, E. Suresh, A binuclear chloride bridged copper(II) complex with a modified ligand structure and different coordination environment and mononuclear cobalt(II) complexes with a pyridylpyrazole ligand: synthesis, structure and cytotoxic activity, Polyhedron 36 (2012) 15–20.
[25] D. Senthil Raja, N.S.P. Bhuvanesh, K. Natarajan, A novel water soluble ligand bridged cobalt(II) coordination polymer of 2-oxo-1,2-dihydroquinoline-3-carbaldehyde (isonicotinic) hydrazone, evaluation of the DNA binding, protein interaction, radical scavenging and anticancer activity, Dalton Trans. 41 (2012) 4365–4377.
[26] S.D. Schimler, D.J. Hall, S.L. Debbert, Anticancer (hexacarbonyldicobalt) propargyl aryl ethers: synthesis, antiproliferative activity, apoptosis induction, and effect on cellular oxidative stress, J. Inorg. Biochem. 119 (2013) 28–37.
[27] M.J.M. Campbell, Transition metal complexes of thiosemicarbazide and thiosemicarbazones, Coord. Chem. Rev. 15 (1975) 279–319.
[28] J.G. Tojal, A.G. Orad, A.A. Diaz, J.L. Serra, M.K. Urtiaga, M.I. Arriortua, T. Rojo, Biological activity of complexes derived from pyridine-2-carbaldehyde thiosemicarbazone: Structure of $[Co(C_7H_7N_4S)_2][NCS]$, J. Inorg. Biochem. 84 (2001) 271–278.
[29] U. El-Ayaan, M.M. Youssef, S. Al-Shihry, Mn(II), Co(II), Zn(II), Fe(III) and U (VI) complexes of 2-acetylpyridine ^4N-(2-pyridyl) thiosemicarbazone (HAPT); structural, spectroscopic and biological studies, J. Mole. Struct. 936 (2009) 213–219.
[30] A.Y. Lukmantara, D.S. Kalinowski, N. Kumar, Des R. Richardson, Synthesis and biological evaluation of substituted 2-benzoylpyridine thiosemicarbazones: novel structure–activity relationships underpinning their anti-proliferative and chelation efficacy, Bioorg. Med. Chem. Lett. 23 (2013) 967–974.
[31] A. Walcourt, M. Loyevsky, D.B. Lovejoy, V.R. Gordeuk, Des R. Richardson, Novel aroylhydrazone and thiosemicarbazone iron chelators with anti-malarial activity against chloroquine-resistant and -sensitive parasites, Int. J. Biochem. Cell Biol. 36 (2004) 401–407.
[32] M. Serda, D.S. Kalinowski, A.M. Wilczkiewicz, R. Musiol, A. Szurko, A. Ratuszna, N. Pantarat, Z. Kovacevic, A.M. Merlot, Des R. Richardson, J. Polanski, Synthesis and characterization of quinoline-based thiosemicarbazones and correlation of cellular iron- binding efficacy to anti-tumor efficacy, Bioorg. Med. Chem. Lett. 22 (2012) 5527–5531.
[33] R. Prabhakaran, P. Kalaivani, P. Poornima, F. Dallemer, G. Paramaguru, V. Vijaya Padma, R. Renganathan, R. Huange, K. Natarajan, One pot synthesis of structurally different mono and dimeric Ni(II) thiosemicarbazone complexes and *N*-arylation on a coordinated ligand: a comparative biological study, Dalton Trans. 41 (2012) 9323–9336.
[34] A.E. Liberta, D.X. West, Antifungal and antitumor activity of heterocyclic thiosemicarbazones and their metal complexes: current status, Biometals 5 (1992) 121–126.
[35] A. Castineiras, D.X. West, H. Gebremedhin, T.J. Romack, Cobalt(III) complexes with 2-acetyl- and 2-formylpyridine ^4N-methylthiosemicarbazones, Inorg. Chim. Acta 216 (1994) 229–236.
[36] D.X. West, J.S. Ives, J. Krejci, M.M. Salberg, T.L. Zumbahlen, G.A. Bain, A.E. Liberta, Copper(II) complexes of 2-benzoylpyridine ^{4}N-substituted thiosemicarbazones, Polyhedron 14 (1995) 2189–2200.
[37] D.X. West, J.K. Swearingena, J.V. Martinez, S.H. Ortega, A.K. El-Sawaf, F. Meursd, A. Castineirase, I. Garciae, E. Bermejoe, Spectral and structural studies of iron(III), cobalt(II, III) and nickel(II) complexes of 2-pyridineformamide N(4)- methyl thiosemicarbazone, Polyhedron 18 (1999) 2919–2929.
[38] D.K. Demertzi, M.A. Demertzis, J.R. Miller, C.S. Frampton, J.P. Jasinski, D.X. West, Structure of bis(2-acetylpyridine 3-hexamethyleneiminyl thiosemicarbazonato) palladium(II), a potential antitumor complex, J. Inorg. Biochem. 92 (2002) 137–140.
[39] R. Manikandan, N. Chitrapriya, Y.J. Jang, P. Viswanathamurthi, Evaluation of DNA- binding, radical scavenging and cytotoxic activity of five coordinated Cd(II) complexes containing 2-acetylpyridine-N4-substituted thiosemicarbazone, RSC Adv. 3 (2013) 11647–11657.
[40] G.N. Rao, Ch. Janardhana, K. Pasupathy, P. Mahesh Kumar, Effect of transition metal complexes on aryl–aryl coupling, Ind. J. Chem. 39B (2000) 151–153.
[41] C.R. Kowol, R. Trondl, P. Heffeter, V.B. Arion, M.A. Jakupec, A. Roller, M. Galanski, W. Berger, B.K. Keppler, Impact of metal coordination on cytotoxicity of 3-amino pyridine-2-carboxaldehyde thiosemicarbazone (Triapine) and novel insights into terminal dimethylation, J. Med. Chem. 52 (2009) 5032–5043.
[42] C.R. Kowol, E. Reisner, I. Chiorescu, V.B. Arion, M. Galanski, D.V. Deubel, B.K. Keppler, An electrochemical study of antineoplastic gallium, iron and ruthenium complexes with redox noninnocent α-N-heterocyclic chalcogensemicarbazones, Inorg. Chem. 47 (2008) 11032–11047.
[43] A. Altomare, G. Cascarano, C. Giacovazzo, A. Guagliardi, M.C. Burla, G. Polidori, M. Camalli, *SIR*92 – a program for automatic solution of crystal structures by direct methods, J. Appl. Crystallogr. 27 (1994) 435–436.
[44] P.T. Beurskens, G. Admiral, G. Beurskens, W.P. Bosman, R. De Gelder, R. Israel, J.M.M. Smits, The DIRDIF-99 Program System, Technical Report of the Crystallography Laboratory, University of Nijmegen, Netherlands, 1999.
[45] J.R. Carruthers, J.S. Rollett, P.W. Betteridge, D. Kinna, L. Pearce, A. Larsen, E. Gabe, Chemical Crystallography Laboratory, UK, Oxford, 1999.
[46] J. Sambrook, E.F. Fritsch, T. Maniatis, Molecular cloning, A laboratory Manual. second ed. Cold Spring, Harbor Laboratory, Cold Spring Harbor, New York, 1989.
[47] M.S. Blois, Antioxidant determination by the use of a stable free radical, Nature 29 (1958) 1199–1200.
[48] T. Nash, The colorimetric estimation of formaldehyde by means of the Hantzsch reaction, Biochem. J. 55 (1953) 416–421.

[49] L.C. Green, D.A. Wagner, J. Glogowski, P.L. Skipper, J.S. Wishnok, S.R. Tannenbaum, Analysis of nitrate, nitrite, and [^{15}N] nitrate in biological fluids, Anal. Biochem. 126 (1982) 131–138.
[50] M. Blagosklong, W.S. El-diery, In vitro evaluation of a p53-expressing adenovirus as an anti-cancer drug, Int. J. Cancer 67 (1996) 386–392.
[51] A. Kumbhar, P. Sonawane, S. Padhye, D.X. West, R.J. Butcher, Structure of antitumor agents 2-acetylpyridinethiosemicarbazone hemihydrate and 2-acetylpyridine thiosemicarbazone hydrochloride, J. Chem. Crystallogr. 27 (1997) 533–539.
[52] M.B. Ferrari, G.G. Fava, M. Lanfranchi, C. Pelizzi, P. Tarasconi, Thiosemicarbazones as co-ordinating agents. Part 4. Synthesis, spectroscopic characterization and X-ray structure of two cobalt(III) complexes with pyridoxal thiosemicarbazone, J. Chem. Soc., Dalton Trans. (1991) 1951–1957.
[53] R. Chikate, P. Sonawane, A. Kumbhar, S. Padhye, R. Butcher, Electrochemical, spectroscopic and structural characterization of the *mer* isomer of ammonium bis(pyruvic acid thiosemicarbazone)cobalt(III)·benzene, Inorg. Chim. Acta 205 (1993) 59–65.
[54] P. Sonawane, R. Chikate, A. Kumbhar, S. Padhye, Inequivalent coordination of thiosemicarbazone ligands in cobalt (III) and chromium (III) complexes, Polyhedron 13 (1994) 395–401.
[55] M.B. Ferrari, G.G. Fava, G. Pelosi, M.C.R. Arguelles, P. Tarasconi, Cobalt(III) complexes with thiosemicarbazones as co-ordinating agents. Spontaneous resolution by crystallization and absolute configuration, J. Chem. Soc., Dalton Trans. (1995) 3035–3040.
[56] S. Pal, S. Pal, Ruthenium(II) complexes containing RuN_4O_2 spheres assembled *via* pyridine- imine-amide coordination. Syntheses, structures, properties and protonation behaviour of coordinated amide, J. Chem. Soc., Dalton Trans. (2002) 2102–2108.
[57] P. Kalaivani, R. Prabhakaran, E. Ramachandran, F. Dallemer, G. Paramagru, R. Renganathan, P. Poornima, V. Vijaya Padma, K. Natarajan, Influence of terminal substitution on structural, DNA, Protein binding, anticancer and antibacterial activities of palladium(II) complexes containing 3-methoxy salicylaldehyde-4(N) substituted thiosemicarbazones, Dalton Trans. 41 (2012) 2486–2499.
[58] T. Sathiya Kamatchi, N. Chitrapriya, H. Lee, C.F. Fronczek, F.R. Fronczek, K. Natarajan, Ruthenium(II)/(III) complexes of 4-hydroxy-pyridine-2,6-dicarboxylic acid with PPh3/AsPh3 as co-ligand, Impact of oxidation state and co-ligands on anticancer activity in vitro, Dalton Trans. 41 (2012) 2066–2077.
[59] S. Satyanarayana, J.C. Dabrowiak, J.B. Chaires, Neither.DELTA.- nor.LAMBDA.-tris(phenanthroline)ruthenium(II) binds to DNA by classical intercalation, Biochemistry 31 (1992) 9319–9324.
[60] Q. Yu, Y. Liu, J. Zhang, F. Yang, D. Sun, D. Liu, Y. Zhou, J. Liu, Ruthenium(II) polypyridyl complexes as G-quadruplex inducing and stabilizing ligands in telomeric DNA, Metallomics 5 (2013) 222–231.
[61] N. Shahabadi, M. Falsafi, N.H. Moghadam, DNA interaction studies of a novel Cu(II) complex as an intercalator containing curcumin and bathophenanthroline ligands, J. Photochem. Photobiol., B 122 (2013) 45–51.
[62] D.S. Raja, G. Paramaguru, N.S.P. Bhuvanesh, J.H. Reibenspies, R. Renganathan, K. Natarajan, Effect of terminal N-substitution in 2-oxo-1,2-dihydroquinoline-3- carbaldehyde thiosemicarbazones on the mode of coordination, structure, interaction with protein, radical scavenging and cytotoxic activity of copper(II) complexes, Dalton Trans. 40 (2011) 4548–4559.
[63] D.S. Raja, N.S.P. Bhuvanesh, K. Natarajan, Biological evaluation of a novel water soluble sulphur bridged binuclear copper(II) thiosemicarbazone complex, Eur. J. Med. Chem. 46 (2011) 4584–4594.
[64] D.S. Raja, N.S.P. Bhuvanesh, K. Natarajan, Synthesis, crystal structure and pharmacological evaluation of two new Cu(II) complexes of 2-oxo-1,2 dihydroquinoline-3- carbaldehyde (benzoyl) hydrazone: a comparative investigation, Eur. J. Med. Chem. 47 (2012) 73–85.
[65] D.S. Raja, N.S.P. Bhuvanesh, K. Natarajan, Effect of N(4)-Phenyl Substitution in 2- Oxo-1,2-dihydroquinoline-3-carbaldehyde Semicarbazones on the Structure, DNA/Protein Interaction, and Antioxidative and Cytotoxic Activity of Cu(II) Complexes, Inorg. Chem. 50 (2011) 12852–12866.
[66] C. Kontogiorgis, D. Hadjipavlou-Litina, Biological evaluation of several coumarin derivatives designed as possible anti-inflammatory/antioxidant agents, J. Enzyme Inhib. Med. Chem. 18 (2003) 63–69.